IEEE Access
Multidisciplinary ⋮ Rapid Review ⋮ Open Access Journal

Received March 11, 2022, accepted March 18, 2022, date of publication March 25, 2022, date of current version April 5, 2022.

Digital Object Identifier 10.1109/ACCESS.2022.3162248

Pin-Gap Correction of Coaxial Calibration Standards for TRL or LRL Calibration

HYUNJI KOO[1], (Member, IEEE), CHIHYUN CHO[1], (Senior Member, IEEE), TAE-WEON KANG[1], (Senior Member, IEEE), AND JAE-YONG KWON[1,2], (Senior Member, IEEE)

[1]Division of Physical Metrology, Electromagnetic Wave Metrology Group, Korea Research Institute of Standards and Science, Daejeon 34113, South Korea
[2]Science of Measurement Department, University of Science and Technology, Daejeon 305350, South Korea

Corresponding author: Hyunji Koo (hyunji.koo@kriss.re.kr)

This work was supported by the Enhancement of Measurement Standards and Technologies in Physics through the Korea Research Institute of Standards and Science under Grant KRISS-2022-GP2022-0002.

ABSTRACT In this paper, a novel method is proposed by which to correct the pin gaps of coaxial calibration standards for Thru-Reflect-Line (TRL) or Line-Reflect-Line (LRL) calibration. This method is a post-process in which the pin-gap correction is applied to the measured S-parameters of the device under test (DUT) after TRL or LRL calibration. It is based on the perturbation equations derived from the sensitivity-coefficient approach. These equations enable us to obtain the correction quantity of the DUT-S-parameter due to the pin gaps. We verify the proposed method by simulation for a 2.4 mm coaxial line, and the result shows that the pin-gap correction works successfully. Because the method is based on the perturbation equations, the smaller the pin gap, the better the correction results. Nevertheless, we can achieve sufficient correction results within the range of the pin-gap to at least 10 times the nominal value. In addition, the proposed pin-gap correction can play the role of impedance renormalization, even though the two LRL calibration lines have different characteristic impedance. Finally, we demonstrate the correction method for a 2.4 mm coaxial LRL calibration kit through measurement.

INDEX TERMS Calibration standard, coaxial, pin-gap correction, impedance renormalization, measurement uncertainty, LRL calibration, TRL calibration.

I. INTRODUCTION

When a male connector and a female connector of a coaxial line are joined, a gap inevitably occurs in the inner conductor due to mechanical tolerance, as shown in Fig. 1. The pin gap is the sum of pin depths on both sides at the reference plane: one is a male pin depth (d_M), and the other is a female pin depth (d_F). Pin gaps in Line-Reflect-Line (LRL) and Thru-Reflect-Line (TRL) calibration standards affect the accuracy of S-parameter measurements. The ideal Line1, Line2, and Reflect for the LRL calibration have the following S-parameter conditions [1],

$$S^{\mathrm{T}} = \begin{bmatrix} 0 & L_1 \\ L_1 & 0 \end{bmatrix}, \quad S^{\mathrm{L}} = \begin{bmatrix} 0 & L_2 \\ L_2 & 0 \end{bmatrix}, S^{\mathrm{R}} = \begin{bmatrix} \Gamma & 0 \\ 0 & \Gamma \end{bmatrix}, \quad (1)$$

where L_1 and L_2 are $e^{-\gamma l_1}$ and $e^{-\gamma l_2}$, respectively. The terms l_1, l_2, and γ are the length of Line1 and Line2, and the propagation constant, respectively. Here, Γ is the reflection coefficient of Reflect. In other words, the ideal lines should have no reflection and should have a reciprocal characteristic ($S_{12} = S_{21}$). The two lines should have the same propagation constant. Moreover, the reflection coefficients of the ideal Reflect should be the same for port1 and port2.

Now, suppose the LRL calibration standards have pin gaps, as shown in Fig. 2. For that case, we present the perturbed S-parameters of the calibration standards that correspond to the S-parameters of the ideal ones given by (1), as follows.

$$S^{\mathrm{T}}_{\mathrm{pert}} = \begin{bmatrix} \delta T_{11} & L_1 + \delta T_{12} \\ L_1 + \delta T_{21} & \delta T_{22} \end{bmatrix},$$
$$S^{\mathrm{L}}_{\mathrm{pert}} = \begin{bmatrix} \delta L_{11} & L_2 + \delta L_{12} \\ L_2 + \delta L_{21} & \delta L_{22} \end{bmatrix},$$
$$S^{\mathrm{R}}_{\mathrm{pert}} = \begin{bmatrix} \Gamma + \delta\Gamma_{11} & 0 \\ 0 & \Gamma + \delta\Gamma_{22} \end{bmatrix}, \quad (2)$$

The associate editor coordinating the review of this manuscript and approving it for publication was Fulvio Schettino.

This work is licensed under a Creative Commons Attribution 4.0 License. For more information, see https://creativecommons.org/licenses/by/4.0/

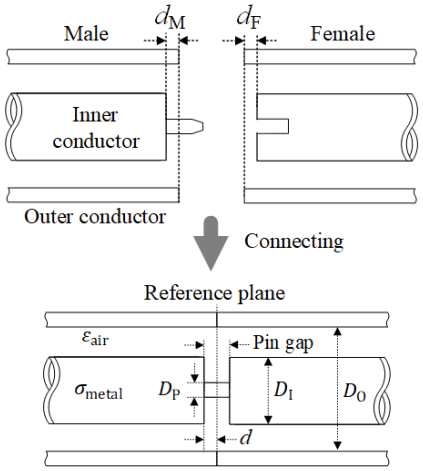

FIGURE 1. A coaxial line connection.

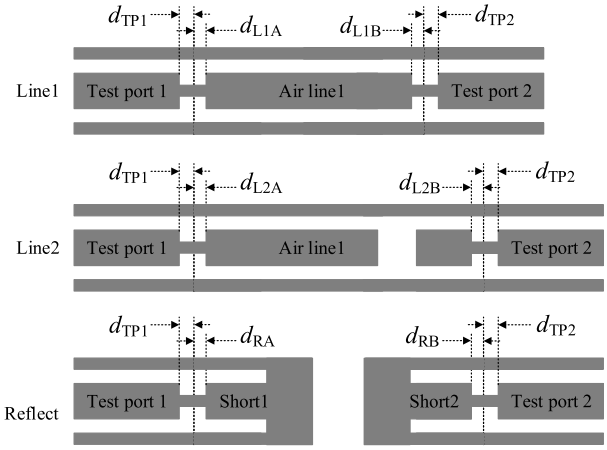

FIGURE 2. The pin gaps of LRL calibration standards.

where δT_{11}, δT_{22} and δT_{12}, δT_{21} are the perturbed reflection coefficients and transmission coefficients of Line1, respectively. The term pairs δL_{11}, δL_{22} and δL_{12}, δL_{21} are the perturbed reflection coefficients and transmission coefficients of Line2, respectively. Here, $\delta\Gamma_1$ and $\delta\Gamma_2$ are the perturbed reflection coefficients of Reflect for port1 and port2, respectively. The ideal and the perturbed S-parameters of the TRL calibration standards can be obtained by setting $L_1 = 1$ in (1) and (2). The perturbed S-parameter of the calibration standards inevitably affects the calibrated S-parameter of the device under test (DUT). Thus, it is necessary to correct the pin gaps.

Several methods have been introduced for pin-gap correction of the calibration standards. In previous work [2], [3], the calibration standards were modeled, including the pin gaps, using a 3D electromagnetic (EM) simulator. A nonlinear fitting process was performed to obtain the error terms. This process is more complicated than the general TRL or LRL calibration. Previous work [4] determined an equivalent standard definition for a vector network analyzer (VNA) calibration model, including the S-parameter of misaligned waveguides. This method removes the effect of the discontinuity occurring in the connections of the waveguide. However, it is difficult to apply this approach directly to coaxial calibration because even pin gaps of a DUT may be considered a non-ideal factor.

In this paper, a novel and simple method is proposed to correct the pin gaps of LRL or TRL coaxial calibration standards. This method corrects the pin-gap effect using perturbation equations after LRL or TRL calibration. These equations were originally derived to obtain S-parameter uncertainty for LRL and TRL calibrations [5]. We verified the proposed correction method by simulation for a 2.4 mm coaxial line [6], [7]. We also found that the pin-gap correction induces impedance renormalization. Finally, we demonstrate the pin-gap correction of the LRL calibration for the 2.4 mm coaxial calibration standards.

The rest of this paper is organized as follows. In Section II, we describe the perturbation equation, which is the basis of the proposed pin-gap correction, and present the correction process. In Section III, we verify the proposed pin-gap correction by simulation. The relationship between pin-gap correction and impedance renormalization is also examined. In Section IV, we demonstrate the pin-gap correction of 2.4 mm LRL calibration standards through measurement. In this paper, we do not consider the influence of the raw values caused by nonlinearity, cross-talk, noise, etc.

We emphasize here that the pin gaps to be corrected indicate only those of the calibration standards. The pin gaps of the DUT, as well as those of the two test ports of a VNA (d_{TP1} and d_{TP2} in Fig. 2), are not corrected using the correction method. This is because the pin gaps of the DUT should be considered inherent characteristics of the DUT, and the pin gaps of the VNA test ports are implicitly included in the error box after calibration [2]. The pin gaps of Line1, Line2, and Reflect used in the LRL calibration are d_{L1A}, d_{L1B}, d_{L2A}, d_{L2B}, d_{RA}, and d_{RB}, respectively, as shown in Fig. 2. For TRL calibration, there is no pin gap for Thru.

II. PROPOSED PIN-GAP CORRECTION

A. PERTURBATION EQUATION

Previous work [1], [5] derived the S-parameter uncertainty equations due to non-ideal LRL or TRL calibration standards. It shows that if we know the amount of the perturbed S-parameters of the calibration standards from the ideal condition, we can calculate the amount of the DUT S-parameters' deviation. Assume that the perturbed S-parameters of Line1, Line2, and Reflect are δT, δL, and δR, respectively. Then, the deviation of the DUT S-parameter, δS_{DUT}, can be obtained using (3) to (8), as shown at the bottom of the next page.

In (3) to (8), $S_{DUT,ij}$ $(i, j = 1, 2)$ is the calibrated DUT S-parameter, $r_{ij} = S_{DUT,ij}/L_1$, $M = L_2/L_1$, and e_{11} is an error term calculated through LRL calibration. The terms including e_{11} in (4) to (7) are negligible [5]. The terms δr^T, δr^L, and δr^R mean δr caused by δT, δL, and δR, respectively. (3) can be

simplified as $\delta S_{\mathrm{DUT},ij} = L_1.\delta r_{ij}$ $(i, j = 1, 2)$, if we assume that the uncertainty of the line length (l_1 and l_2) is zero. The terms $\delta r_{21}^{\mathrm{T}}$, $\delta r_{22}^{\mathrm{T}}$, $\delta r_{21}^{\mathrm{L}}$, and $\delta r_{22}^{\mathrm{L}}$ can be determined by exchanging the index 1 with 2 in (4) to (7). Interestingly, these equations show that δL_{12} and δL_{21} do not change the DUT S-parameters and δR only affects the reflection coefficients of the DUT.

For the TRL calibration, $L_1 = 1$ (Thru), $r_{ij} = S_{\mathrm{DUT},ij}$, $\delta r_{ij} = \delta S_{\mathrm{DUT,ij}}$ $(i, j = 1, 2)$, and $M = L_2$ (Line) in (3) to (8).

B. PIN-GAP CORRECTION

Here, we propose a new method for pin-gap correction using the above perturbation equations. This is achieved by considering the pin gaps of the calibration standards as non-ideal factors. First, we measure the raw S-parameters of the LRL or TRL calibration standards and a DUT. Then, we obtain the DUT S-parameters (S_{DUT}), the propagation constant γ of the lines and error term e_{11} using a general LRL or TRL calibration algorithm. Then, we define ideal line standards without pin gaps ($S^{\mathrm{T}}_{\mathrm{w/o\_gap}}, S^{\mathrm{L}}_{\mathrm{w/o\_gap}}$) using γ and their lengths based on (1). We also model the calibration standards with pin gaps ($S^{\mathrm{T}}_{\mathrm{w/gap}}$, $S^{\mathrm{L}}_{\mathrm{w/gap}}$, and $S^{\mathrm{R}}_{\mathrm{w/gap}}$) based on the dimensional measurement. Next, we calculate the perturbed S-parameters of the calibration standards (δT, δL, and δR) by using the following equations,

$$\begin{bmatrix} \delta T_{11} & \delta T_{12} \\ \delta T_{21} & \delta T_{22} \end{bmatrix} = S^{\mathrm{T}}_{\mathrm{w/gap}} - S^{\mathrm{T}}_{\mathrm{w/o\_gap}},$$
$$\begin{bmatrix} \delta L_{11} & \delta L_{12} \\ \delta L_{21} & \delta L_{22} \end{bmatrix} = S^{\mathrm{L}}_{\mathrm{w/gap}} - S^{\mathrm{L}}_{\mathrm{w/o\_gap}},$$
$$\delta R = \left(S^{\mathrm{R}}_{\mathrm{w/gap}}\right)_{22} - \left(S^{\mathrm{R}}_{\mathrm{w/gap}}\right)_{11}. \quad (9)$$

Then, we calculate the perturbed S-parameters of the DUT $\delta S^{\mathrm{T}}_{,}\delta S^{\mathrm{L}}_{,}$ and δS^{R}(from δr^{T}, δr^{L}, and δr^{R}, respectively) through (3) to (8). Finally, we obtain the pin-gap corrected S-parameters of the DUT $S_{\mathrm{DUT\_corr}}$ using (10).

$$S_{\mathrm{DUT\_corr}} = S_{\mathrm{DUT}} - \delta S^{\mathrm{T}} - \delta S^{\mathrm{L}} - \delta S^{\mathrm{R}}. \quad (10)$$

(10) indicates that the pin-gap correction of each calibration standard is independently applied to S_{DUT}. Practically, this makes it easy to replace a fault-calibration standard with a normal one by evaluating only the fault-calibration one. The whole process is summarized in Fig. 3.

III. VERIFICATION BY SIMULATION

A. MODELING OF COAXIAL CALIBRATION STANDARDS AND DUT

To verify the proposed pin-gap correction, we modeled the 2.4 mm coaxial calibration standards, the Beatty line as a DUT, and the VNA error box, using [6], [7]. The simulation parameters used for modeling are the diameter of the inner and outer conductors (D_{I}, D_{O}), pin diameter (D_{P}), pin depth (d), the conductivity of the conductor (σ_{metal}), and the relative permittivity of air ($\varepsilon_{\mathrm{air}}$), as shown in Fig. 1. Table 1 shows the values of the parameters, referring to [6].

We set the lengths of Line1 and Line2 as 12.5 and 15 mm, respectively. The pin depths of Line1 and Line2 are set as 0.0065 mm, a manufacturer's nominal value for metrology grade coaxial connectors. The pin depths of Reflect on both ports were set to 0.0065 and 0.0130 mm, respectively. Error boxes were also modeled using coaxial lines of which the characteristic impedance deviated from 50 Ω.

Fig. 4 presents the Beatty line configuration and its S-parameters. The figure also includes the pin gaps (d_{DUTA} and d_{DUTB}) of 0.0065 mm. The Beatty line enables

$$\delta S_{\mathrm{DUT},ij} = L_1 \cdot \delta r_{ij} + S_{\mathrm{DUT},ij} \cdot \left[\frac{l_1}{l_2 - l_1} \cdot \frac{\delta M}{M} + \ln(M)\frac{l_2\delta l_1 - l_1\delta l_2}{(l_2 - l_1)^2}\right], \quad (i, j = 1, 2) \quad (3)$$

$$\delta r_{11}^{\mathrm{T}} = \left\{\frac{M^2 - r_{12}r_{21}}{(1 - M^2)\cdot L_1}\delta T_{11} - \frac{r_{11}(\Gamma^2 + L_1^2M^2)}{2L_1^2(1 - M^2)\cdot\Gamma}(\delta T_{11} - \delta T_{22}) - \frac{r_{11}}{2\cdot L_1}(\delta T_{12} + \delta T_{21}) + \frac{M^2\cdot e_{11}}{(1 - M^2)}\right.$$
$$\left.\cdot\left[\frac{r_{11}(\Gamma^2 + L_1^2)}{2\cdot L_1\cdot\Gamma} - r_{11}^2\right]\cdot(\delta T_{12} - \delta T_{21}) - \frac{r_{11}^2}{L_1\cdot(1 - M^2)}\cdot\delta T_{22}\right\} \quad (4)$$

$$\frac{\delta r_{12}^{\mathrm{T}}}{r_{12}} = -\frac{r_{22}}{L_1\cdot(1 - M^2)}\delta T_{11} - \frac{1}{L_1}\delta T_{12} - \frac{r_{11}\cdot M^2\cdot e_{11}}{(1 - M^2)}(\delta T_{12} - \delta T_{21}) - \frac{r_{11}}{L_1\cdot(1 - M^2)}\cdot\delta T_{22}, \quad (5)$$

$$\delta r_{11}^{\mathrm{L}} \approx \left\{-\frac{1 - r_{21}r_{12}}{L_1\cdot(1 - M^2)}\delta L_{11} + \frac{r_{11}(\Gamma^2 + L_1^2)}{2\cdot L_1^2\cdot(1 - M^2)\cdot\Gamma}(\delta L_{11} - \delta L_{22}) - \frac{M^2\cdot e_{11}}{(1 - M^2)}\cdot\left[\frac{r_{11}(\Gamma^2 + L_1^2)}{2\cdot L_1\cdot\Gamma} - r_{11}^2\right]\right.$$
$$\left.\cdot(\delta L_{12} - \delta L_{21}) + \frac{r_{11}^2}{L_1\cdot(1 - M^2)}\cdot\delta L_{22}\right\}, \quad (6)$$

$$\frac{\delta r_{12}^{\mathrm{L}}}{r_{12}} = \frac{r_{22}}{L_1\cdot(1 - M^2)}\delta L_{11} + \frac{r_{11}\cdot M\cdot e_{11}}{(1 - M^2)}(\delta L_{12} - \delta L_{21}) + \frac{r_{11}}{L_1\cdot(1 - M^2)}\cdot\delta L_{22}, \quad (7)$$

$$\delta r_{11}^{\mathrm{R}} = \frac{r_{11}}{2\cdot\Gamma}\delta R, \quad \delta r_{22}^{\mathrm{R}} = -\frac{r_{22}}{2\cdot\Gamma}\delta R \quad (8)$$

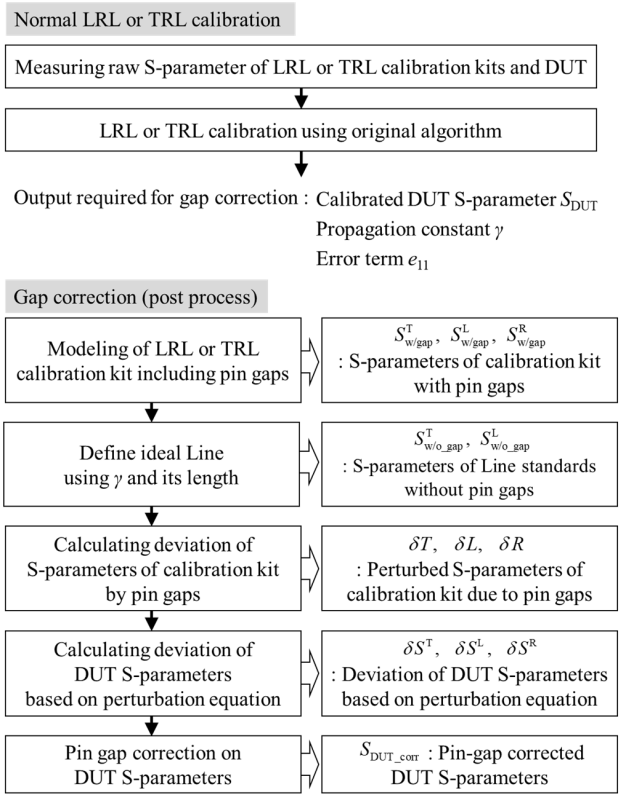

FIGURE 3. The process of the proposed pin-gap correction.

TABLE 1. Simulation parameters of 2.4 mm coaxial standards.

Parameter (units)	Symbol	Value
Outer conductor diameter (mm)	D_O	2.4
Inner conductor diameter (mm)	D_I	1.0423
Pin diameter (mm)	D_P	0.511
Pin depth (mm)	d	0.0065
Metal Conductivity (S/m)	σ_{metal}	6×10^{6}
Relative Dielectric Constant	ε_{air}	1
Dielectric Loss Tangent	-	0

us to investigate the corrected results in both impedance matching and mismatching conditions.

B. PIN-GAP CORRECTED RESULTS

Because we modeled the DUT, we know its exact S-parameter, S_{DUT_ideal}. After the LRL or TRL calibration, we obtained S_{DUT_LRL}, which is different from S_{DUT_ideal} due to non-ideal factors like the pin gaps of the calibration standards. We applied the proposed pin-gap correction to S_{DUT_LRL} and obtained the corrected S-parameters of the DUT S_{DUT_corr}.

We compared the performance of the proposed method to that of applying only the LRL (or TRL) calibration algorithm. Fig. 5 shows the errors of the LRL calibration algorithm with and without the pin-gap correction. The errors are obtained

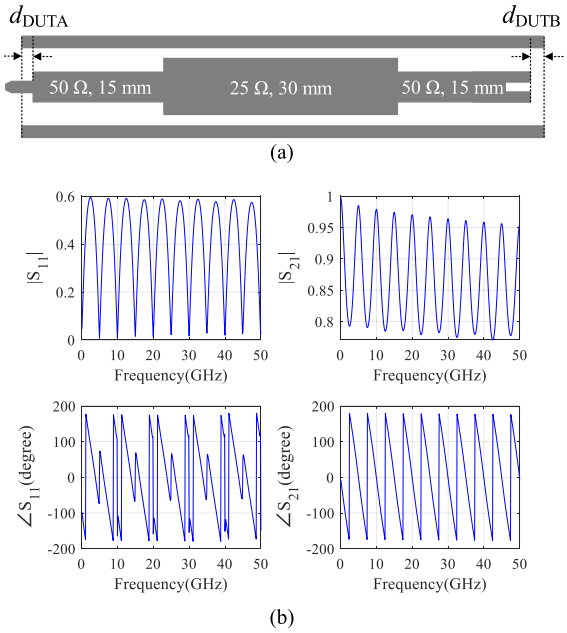

FIGURE 4. Beatty line under test. (a) configuration and (b) its S-parameters.

from the difference between S_{DUT_ideal} and S_{DUT_LRL} and the difference between S_{DUT_ideal} and S_{DUT_corr}.

The magnitude error $\Delta|S|$ and the phase error $\Delta\angle(S)$ of the LRL calibration algorithm without the correction increase to 0.01, and more than 2°, respectively. In particular, the phase discontinuity of the Beatty line makes large peaks in the phase error. However, both the amplitude error and the phase error corrected by the proposed method (red lines), are close to zero. It clearly indicates that the proposed method works well on the pin-gap correction.

We examined the impact of pin gaps for each calibration standard on the DUT S-parameter. The nominal pin gaps of 0.0065 mm for Line1 and Line2 change the magnitude of DUT S-parameters by 0.001-0.005, and the phase up to 2°. The pin gaps in Reflect only affect the phase of DUT S_{11} and S_{22}, and their amount is about 0.3°.

Next, we investigated whether the pin-gap correction works well even when all the pin gaps of calibration standards have an arbitrary pin-gap size within the uncertainty range. We assumed that the uncertainty of the pin-gap size is ±0.0065 mm, and its distribution is rectangular. Fig. 6 shows the simulation results for 100 LRL calibration standards with arbitrary pin-gap sizes. The errors with the pin-gap correction are all close to zero. This shows that the pin-gap correction is well achieved if we know the perturbation value of the S-parameters (δT, δL, and δR) caused by the arbitrary value of the pin gaps. S_{22} and S_{12} are equal to S_{11} and S_{21}, respectively.

In the case of TRL calibration, only the pin gaps in a Line and a Reflect affect the DUT S-parameters. Thus, the errors of the TRL calibration algorithm are smaller than the errors of the LRL calibration algorithm.

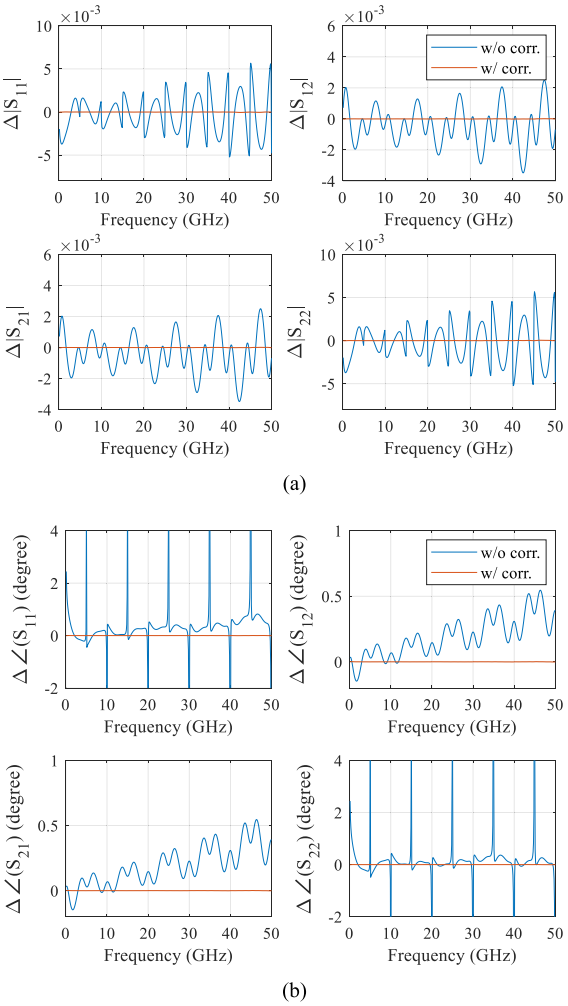

FIGURE 5. Comparison of (a) the magnitude and (b) phase errors of the simulated S-parameters of the Beatty line when using the LRL calibration algorithm with and without the pin-gap correction.

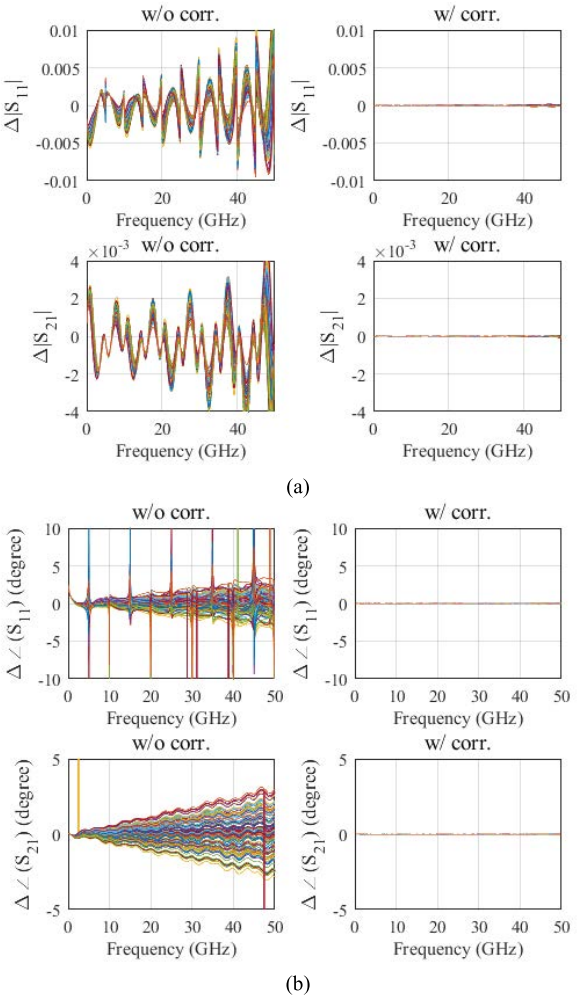

FIGURE 6. Comparison of (a) the magnitude and (b) phase errors of the simulated S-parameters of the Beatty line when using the LRL calibration algorithm with and without the pin-gap correction using 100 random sets of pin-gap size.

C. ALLOWABLE RANGE OF PIN GAP

Because the pin-gap correction is based on the perturbation equation, only small S-parameter changes of the calibration standards can be corrected. Therefore, as the pin gap increases, the correction might not be sufficiently accomplished. Fig. 7 shows plots of the errors of the LRL calibration algorithm with and without the pin-gap correction when the pin gaps of the calibration standards are increased from 2 to 10 times the nominal value (6.5 μm). It shows that the larger the pin-gap size, the more the errors with the pin-gap correction deviate from 0, especially above 40 GHz. It means that the pin-gap correction is not done well. When the pin gap is ten times the nominal value, the maximum $\Delta|S_{11}|$ and $\Delta|S_{21}|$ with the pin-gap correction are 0.004 and 0.0007, respectively. The maximum $\Delta\angle(S_{11})$ and $\Delta\angle(S_{21})$ with the pin-gap correction are 0.77° and 0.07°, respectively. However, applying the correction can still improve the measurement result significantly compared to the results without the correction at ten times the pin gap.

The DUT S-parameter also affects the results. This is because the error of the LRL (or TRL) calibration algorithm is a function of the DUT S-parameter, as shown in (3)-(8). For example, the large $|S_{21}|$ of a DUT increases the errors of the LRL (or TRL) calibration algorithm according to (5) and (7), and correspondingly the errors with the pin-gap correction increases. We confirmed by simulation that the errors with the pin-gap correction have large values in the order of the Thru, the 5 dB attenuator, and the 10 dB attenuator. This shows that low-loss DUTs are more susceptible to the pin-gap effect.

D. IMPEDANCE RENORMALIZATION USING PIN-GAP CORRECTION EQUATIONS

After the TRL or LRL calibration, the reference plane is normalized to Z_C, the characteristic impedance of the Line. This is because the Line is assumed not to have reflection during the calibration. Therefore, we need to renormalize the calibrated S-parameters from Z_C to 50 Ω.

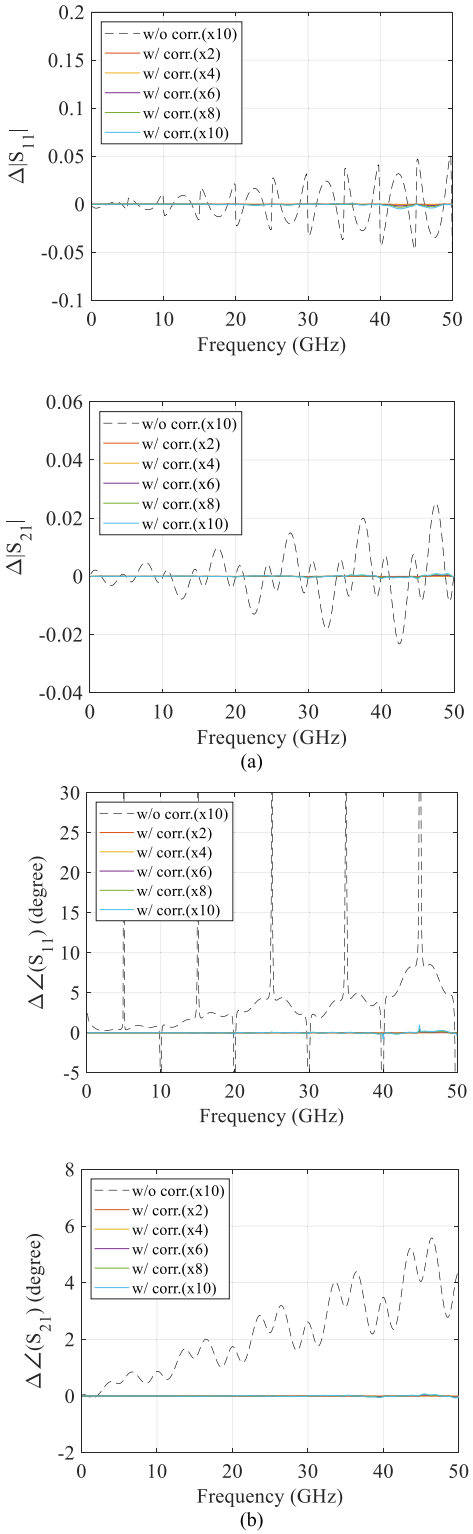

FIGURE 7. Comparison of (a) the magnitude and (b) phase errors of the simulated S-parameters of the Beatty line when using the LRL calibration algorithm with and without the pin-gap correction. Errors with the correction are presented for the pin-gap size from 2 times to 10 times the nominal value (6.5 μm) and errors without the correction are shown for the pin-gap size of 10 times the nominal value.

This renormalization is usually done in the same way as the previous works [8], [9].

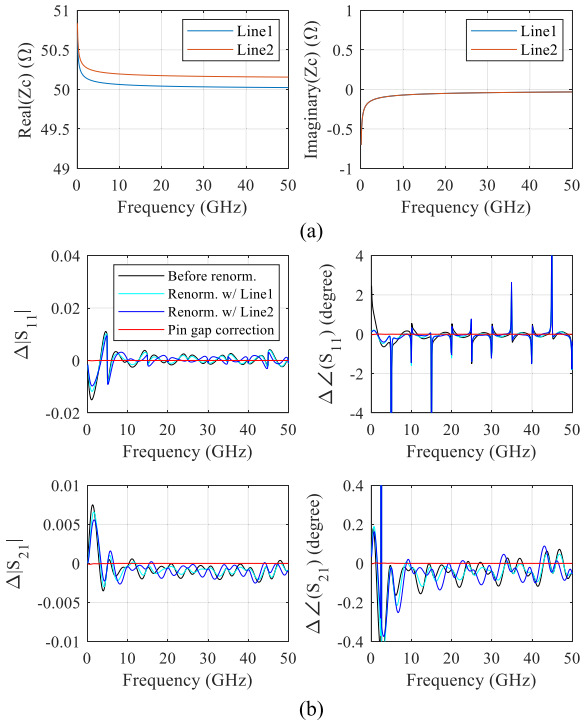

FIGURE 8. The characteristic impedance of lines and comparison of the simulated S-parameters errors of Beatty line. (a) The characteristic impedance of modeled Line1 and Line2. (b) The errors without and with renormalization based on two renormalization methods: the conventional method [8], [9] and the pin-gap correction method. For the conventional method, each characteristic impedance of Line1 and Line2 is used.

The presence of a pin gap in a Line causes the Line impedance as seen from the reference plane to deviate from 50 Ω. This means that reference impedance deviates from 50 Ω. However, the pin-gap corrected result ($S_{\text{DUT\_corr}}$) agrees well with the result defined by the 50 Ω reference impedance ($S_{\text{DUT\_ideal}}$). In this respect, it can be considered that pin-gap correction plays the role of impedance renormalization. This indicates that we can use the pin-gap correction equations for impedance renormalization.

In the correction, we regard the presence of reflection coefficients in the Line as a non-ideal condition, and set the reflection coefficients of the ideal Line to all zeroes in the pin-gap correction. That is, the corrected DUT S-parameter becomes the result of using a line with no reflection in a 50 Ω transmission line, which is a perfect 50 Ω Line.

We verify the impedance renormalization based on the pin-gap correction equations in the LRL calibration. We modeled Line1 and Line2 with different characteristic impedances by adjusting the diameter of the inner conductors, as shown in Fig. 8 (a). First, we carried out impedance renormalization based on [8] and [9] with each characteristic impedance of Line1 and Line2. For this simulation, we set all the pin gaps as 0. Fig. 8 (b) shows the results, which are marked with blue and light blue lines. Both renormalized results are apart from the exact values of the DUT, which means that the impedance renormalizations failed. The impedance of the reference plane is not equal to both characteristic impedances of the two lines.

Second, we applied the pin-gap correction equations for the impedance renormalization. The red lines in Fig. 8 (b) show the results, almost identical to the exact value of the DUT. This indicates that the pin-gap correction can play the role of impedance renormalization. This method allows impedance renormalization even if the characteristic impedances of the two LRL lines are not the same.

If Line1 and Line2 include the pin gaps, and their characteristic impedances deviate from 50 Ω, we can achieve the pin-gap correction and the impedance renormalization at the same time. However, as we have seen in the previous section, the correction is possible only for small errors. If the characteristic impedance deviates considerably from 50 Ω, impedance renormalization will not be done properly. We need further studies about the allowable impedance range.

IV. MEASUREMENT

We demonstrated the pin-gap correction using a 2.4 mm coaxial LRL calibration standards customer-customized by Rosenberger. It consists of flush shorts (male and female) and three airlines 18.6, 20.6, or 25.6 mm long (airline1, airline2, airline3), respectively. We used airline1 and airline2 (length difference of 2 mm) for the frequency band from 100 MHz to 50 GHz, and airline2 and airline3 (length difference of 5 mm) for the frequency band between 100 MHz and 25 GHz.

We connected the female of the airline to test port 1 (port1) of the VNA, and the male to test port 2 (port2), respectively, as shown in Fig. 9(a). We inserted a 25 μm- thick dielectric Kapton ring between the test port 1 and the female connector of the airline to prevent resonance caused by the two inner conductors being too close together [10]. We also measured the Reflect and the DUT with the Kapton ring. The reference plane is shifted to the end of the ring. Thus, there was no requirement to compensate for the effect of the inserted dielectric ring. For the pin-gap correction, we need δT, δL, and δR, which are from the differences of $S_{\mathrm{w/o\_gap}}$ and $S_{\mathrm{w/gap}}$.

First, we calculate $S_{\mathrm{w/o\_gap}}$ using the propagation constant γ obtained by LRL calibration and the length (l_1, l_2, l_3) measured by a tactile measuring probe [11]. The measured values are summarized in Table 2.

Next, we obtain $S_{\mathrm{w/gap}}$ from the dimensions of the airline by dividing it into three parts, as shown in Fig. 9(a). The connectors (part1 and part3) of the airline are modeled using the HFSS 3D EM simulator. The structures of the connectors are presented in Fig. 9 (b). The female inner conductor has four slots. The slot length (sl) and slot width (sw) were measured using a high-resolution vision measuring machine. The pin gaps of male connectors (pg_1, pg_2, pg_3) were measured using a pin-depth gauge, and other parameters are referred to [12]. The detailed parameters are shown in Table 2. The diameters of inner and outer conductors (part2) were measured every 0.1 mm along the length using an LED-micrometer system and a non-contact compressed-air measuring system [10]. Fig. 9(c) shows one of the measurement results and uncertainties for the airlines used. Then, we obtained the S-parameters every 0.1 mm using the Daywitt model [13] and cascaded

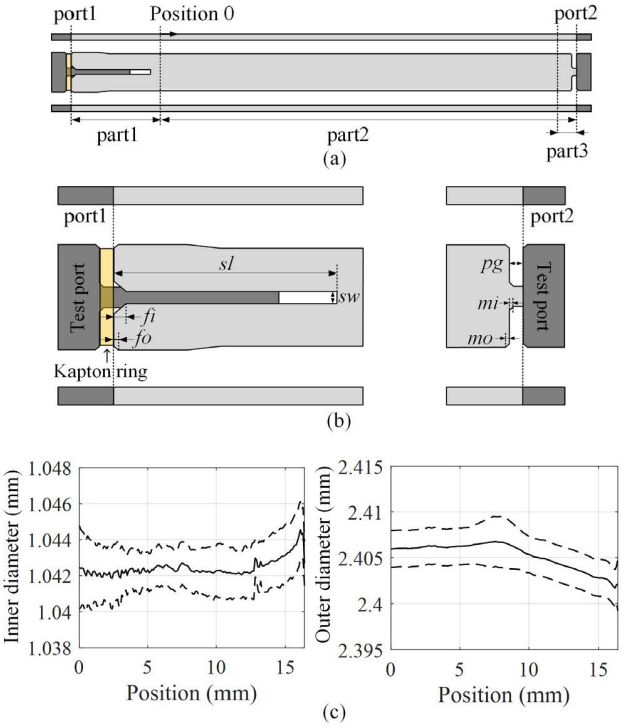

FIGURE 9. An airline connected to test ports. (a) overall configuration, (b) female and male connectors, part1 and part3 of this figure (a), and (c) the measured diameter of inner and outer conductors of airline1, part2 of this figure (a).

TABLE 2. Dimensions of airlines.

Parameter (units)	Symbol	Value
Length of airline1 (mm)	l_1	18.610
Length of airline2 (mm)	l_2	20.609
Length of airline3 (mm)	l_3	25.608
Slot length (mm)	sl	1.84
Slot width (mm)	sw	0.095
Female outer chamfer (μm)	fo	15
Female inner chamfer (μm)	fi	50
Male outer chamfer (μm)	mo	15
Male inner chamfer (μm)	mi	15
Pin gap of airline1 (μm)	pg_1	3.43
Pin gap of airline2 (μm)	pg_2	5.46
Pin gap of airline3 (μm)	pg_3	4.70

them to obtain the S-parameter of part2. Finally, by cascading part1, part2, and part3, we determined the S-parameter of the entire airline. Since we used flush shorts, we did not perform pin-gap correction on the Reflect. However, pin-gap correction can be individually performed on each port depending on the Reflect used.

Note that the obtained propagation constant γ using the LRL has measurement uncertainty due to random errors on the VNA, cable movement, connector repeatability, etc.

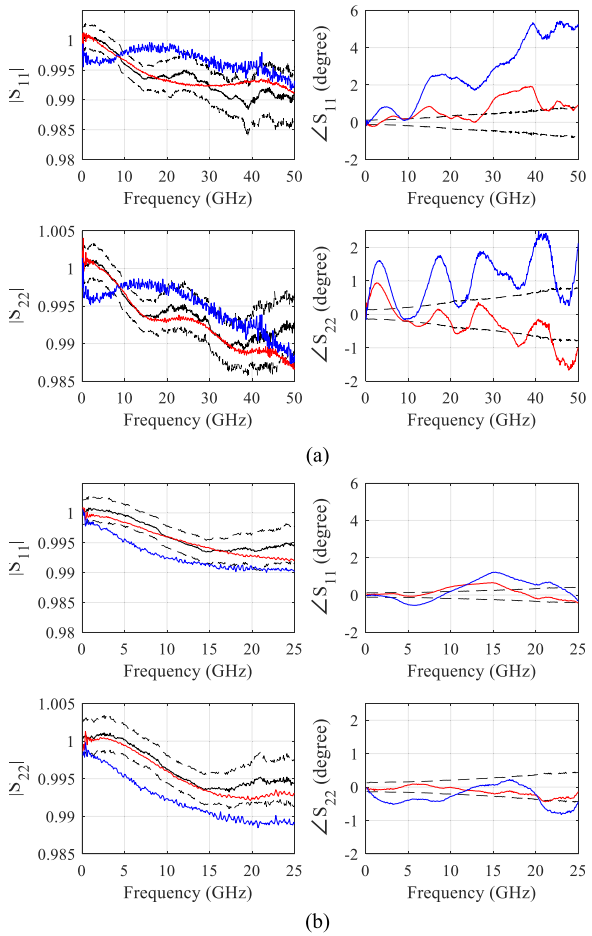

FIGURE 10. The magnitude and phase of the measured S-parameters of Open with (red) and without (blue) pin-gap correction, and evaluated results (black) with the calibration kit calibrated at the Federal Institute of Metrology, METAS, Swiss. (a) Results using airline1 and airline2 and (b) results using airline2 and airline3.

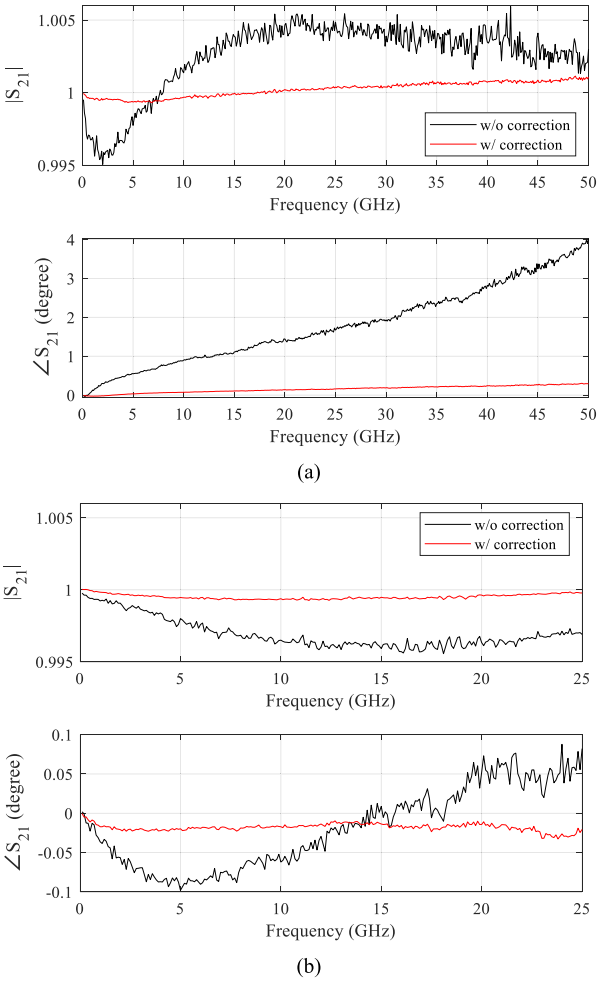

FIGURE 11. The magnitude and phase of the measured S_{21} of Thru under test with (red) and without (black) pin-gap correction. (a) Results using airline1 and airline2 and (b) results using airline2 and airline3.

Moreover, the measured dimensions produce errors on the calculated S-parameters due to measurement uncertainty. We found that the proposed pin-gap correction algorithm can work well even with 0.5% error of the propagation constant and 2.5 μm error of each dimensional measurement. We will analyze the uncertainty later. On calculation of the S-parameters of the connector, we set the mesh size of the EM simulator to be very small (ΔS, the amount of S-parameter change according to mesh increase, $\leq 5 \times 10^{-5}$). Above all, the size of the connector is small compared to the other parts. Thus, this EM simulation error may not significantly affect the pin gap correction.

We demonstrated the proposed pin-gap correction using Open and Thru as DUTs. Fig. 10 shows the magnitude and phase of the measured S-parameters of Open with (red) and without (blue) pin-gap correction. We compared the measured results to the results (black) evaluated using the calibration kit, which was calibrated by the Federal Institute of Metrology, METAS, Swiss. In METAS, the VNA error terms were over-determined based on all the dimensions of the coaxial lines. This approach is known to be the most accurate [2]. The dotted black line shows the uncertainty of the evaluated results. Fig. 10 (a) shows the results using airline1 and airline2 at up to 50 GHz and Fig. 10 (b) shows the results using airline2 and airline3 at up to 25 GHz. The phase of the measured result was normalized to the phase of the evaluated result.

The blue-line results (without pin-gap correction) of Fig. 10 (b) are closer to the evaluated values than those of (a) because the lengths of the airlines in Fig. 10 (b) are suitable for the frequency band. Nevertheless, the red-line results of Fig. 10 (b) show that pin-gap correction can improve the result. The red-line results of Fig. 10 (a) also show the improved results over the entire frequency band. In particular, even at low frequencies, the magnitudes of the S-parameters are improved as much as the results obtained with airlines of proper length after the pin-gap correction. The corrected results of $|S_{11}|$ and $|S_{22}|$ are slightly greater than 1 when at low frequency. This may be due to the length of the airline since the TRL works well when its electrical length is between 20° and 160° [5].

Fig. 11 shows the measured S_{21} of Thru. The magnitude and phase of an ideal Thru S_{21} should be 1 and 0°, respectively. However, the magnitude of S_{21} deviates by 0.005, and the phase deviates by 4° at 50 GHz without the correction, as shown in Fig. 11 (a). After the correction, the deviated magnitude and the phase decreases to $\leq$0.001 and $\leq$0.3°, respectively. Both magnitude and phase are well-improved compared to the results without correction. Using a line of appropriate length, as shown in Fig. 11 (b), the phase without the pin-gap correction shows a value of 0.1° or less, but it can be further improved to about 0.03° through the pin-gap correction. We would be able to reduce the residual errors on the pin-gap corrected S-parameters using more precise data such as the propagation constant γ and measured dimensions.

V. CONCLUSION

In this paper, a novel method to correct pin gaps of coaxial calibration standards for Thru-Reflect-Line (TRL) or Line-Reflect-Line (LRL) calibration was presented. This correction was achieved using perturbation equations, which represent the relationship between the S-parameter perturbation of the calibration standards and the S-parameter deviation of the DUT. By precisely evaluating the S-parameter perturbation of the calibration standards due to the pin gaps, we could obtain the S-parameter deviation of the DUT. Because the pin-gap correction is based on perturbation equations, a considerably large value of the pin gap disables an appropriate correction. Nevertheless, we can achieve sufficient correction results within the range of the pin-gap to at least ten times the nominal value. We also showed that the pin-gap correction could play the role of impedance renormalization. Even though the two Lines of the LRL calibration kit have different characteristic impedances, renormalization could be achieved using the pin-gap correction equations. Finally, the correction was demonstrated using a 2.4 mm coaxial LRL calibration kit through measurement.

This method is more straightforward than the previous approach in that it uses the general LRL or TRL algorithm. In addition, the proposed method is a faster one in which the pin-gap correction is completed within a few seconds, compared to the METAS method, which takes about 12 hours.

In the future, we will evaluate the uncertainty of this method considering the uncertainty of length and cross-sectional dimensions and examine the impedance range that can be renormalized.

REFERENCES

[1] U. Stumper, "Influence of nonideal LRL or TRL calibration elements on VNA S-parameter measurements," *Adv. Radio Sci.*, vol. 3, no. 3, pp. 51–58, May 2005, doi: 10.5194/ars-3-51-2005.

[2] M. Zeier, J. Hoffmann, P. Hürlimann, J. Rüfenacht, D. Stalder, and M. Wollensack, "Establishing traceability for the measurement of scattering parameters in coaxial line systems," *Metrologia*, vol. 55, no. 1, pp. S23–S36, Feb. 2018, doi: 10.1088/1681-7575/aaa21c.

[3] J. Hoffmann, M. Wollensack, J. Ruefenacht, and M. Zeier, "Extended S-parameters for imperfect test ports," *Metrologia*, vol. 52, no. 1, pp. 121–129, Feb. 2015, doi: 10.1088/0026-1394/52/1/121.

[4] D. F. Williams, "Rectangular-waveguide vector-network-analyzer calibrations with imperfect test ports," in *Proc. 76th ARFTG Microw. Meas. Conf.*, Dec. 2010, pp. 1–8, doi: 10.1109/ARFTG76.2010.5700048.

[5] U. Stumper, "Uncertainty of VNA S-parameter measurement due to non-ideal TRL calibration items," *IEEE Trans. Inst. Meas.*, vol. 54, no. 2, pp. 676–679, Apr. 2005, doi: 10.1109/TIM.2005.843521.

[6] J. A. Jargon, C. Cho, D. F. Williams, and P. D. Hale, "Physical models for 2.4 mm and 3.5 mm coaxial VNA calibration kits developed within the NIST microwave uncertainty framework," in *Proc. 85th Microw. Meas. Conf. (ARFTG)*, May 2015, pp. 1–7, doi: 10.1109/ARFTG.2015.7162913.

[7] C. Cho, J.-S. Kang, J.-G. Lee, and H. Koo, "Characterization of a 1 mm (DC to 110 GHz) calibration kit for VNA," *J. Electromagn. Eng. Sci.*, vol. 19, no. 4, pp. 272–278, Oct. 2019, doi: 10.26866/jees.2019.19.4.272.

[8] J. C. Tippet and R. A. Speciale, "A rigorous technique for measuring the scattering matrix of a multiport device with a 2-port network analyzer," *IEEE Trans. Microw. Theory Techn.*, vol. MTT-30, no. 5, pp. 661–666, May 1982, doi: 10.1109/TMTT.1982.1131118.

[9] H. Dropkin, "Comments on 'A rigorous techique for measuring the scattering matrix of a multiport device with a two-port network analyzer,'" *IEEE Trans. Microw. Theory Techn.*, vol. MTT-31, no. 1, pp. 79–81, Jan. 1983, doi: 10.1109/TMTT.1983.1131435.

[10] J. P. Hoffmann, J. Ruefenacht, M. Wollensack, and M. Zeier, "Comparison of 1.85 mm line reflect line and offset short calibration," in *Proc. 76th ARFTG Microw. Meas. Conf.*, Nov. 2010, pp. 1–7, doi: 10.1109/ARFTG76.2010.5700047.

[11] M. Horibe, M. Shida, and K. Komiyama, "Development of evaluation techniques for air lines in 3.5- and 1.0-mm line sizes," *IEEE Trans. Instrum. Meas.*, vol. 58, no. 4, pp. 1078–1083, Apr. 2009, doi: 10.1109/TIM.2008.2008084.

[12] J. Hoffmann and P. Huerlimann, "Key parameters of coaxial connector models—Mechanical design features and electrical properties," Federal Inst. Metrol. (METAS), Switzerland, 2015, pp. 1–30. [Online]. Available: https://www.metas.ch/dam/metas/de/data/Fachbereiche/Hochfrequenz/Documents/hoffmann2015a-coaxconnectors.pdf.download.pdf/hoffmann2015a-coaxconnectors.pdf

[13] W. C. Daywitt, "First-order symmetric modes for a slightly lossy coaxial transmission line," *IEEE Trans. Microw. Theory Techn.*, vol. 38, no. 11, pp. 1644–1650, Nov. 1990, doi: 10.1109/22.60011.

HYUNJI KOO (Member, IEEE) received the B.S. and Ph.D. degrees in electrical engineering from the Korea Advanced Institute of Science and Technology (KAIST), Daejeon, South Korea, in 2008 and 2015, respectively. From March to August 2015, she was a Postdoctoral Research Fellow at the School of Electrical Engineering, KAIST. Since September 2015, she has been a Senior Research Scientist with the Electromagnetic Wave Metrology Group, the Korea Research Institute of Standards and Science (KRISS), Daejeon. In 2018, she was a Visiting Researcher at the National Physical Laboratory (NPL), Teddington, U.K. Her current research interest includes the characterization of on-wafer devices.

CHIHYUN CHO (Senior Member, IEEE) received the B.S., M.S., and Ph.D. degrees in electronic and electrical engineering from Hongik University, Seoul, South Korea, in 2004, 2006, and 2009, respectively. From 2009 to 2012, he participated in the development of military communication systems at the Communication Research and Development Center, Samsung Thales, Bundang-gu, Seongnam, South Korea. Since 2012, he has been with the Korea Research Institute of Standards and Science (KRISS), Daejeon, South Korea. In 2014, he was a Guest Researcher at the National Institute of Standards and Technology (NIST), Boulder, CO, USA. He also served on the Presidential Advisory Council on Science and Technology (PACST), Seoul, from 2016 to 2017. His current research interests include microwave metrology, time-domain measurement, and standard of communication parameters.

TAE-WEON KANG (Senior Member, IEEE) received the B.S. degree in electronic engineering from Kyungpook National University, Daegu, South Korea, in 1988, and the M.S. and Ph.D. degrees in electronic and electrical engineering from the Pohang University of Science and Technology (POSTECH), Pohang, South Korea, in 1990 and 2001, respectively.

Since 1990, he has been with the Division of Physical Metrology, Center for Electromagnetic Metrology, Korea Research Institute of Standards and Science, Daejeon, South Korea, working on the electromagnetic metrology, where he is a Principal Research Scientist. In 2002, he had spent a year as a Visiting Researcher under the Korea Science and Engineering Foundation Postdoctoral Fellowship Program at the George Green Institute for Electromagnetics Research, University of Nottingham, Nottingham, U.K., where he worked on measurement of absorbing performance of electromagnetic absorbers and on a generalized transmission line modeling method. His research interests include numerical modeling in electromagnetic compatibility and electromagnetic metrology, such as electromagnetic power, noise, RF voltage, impedance, and antenna characteristics. He received the Outstanding Researcher Award from the Korean Institute of Electromagnetic Engineering and Science (KIEES), in 2017. Since 2018, he has been an Associate Editor of the IEEE TRANSACTIONS ON INSTRUMENTATION AND MEASUREMENT.

JAE-YONG KWON (Senior Member, IEEE) received the B.S. degree in electronics from Kyungpook National University, Daegu, in 1995, and the M.S. and Ph.D. degrees in electrical engineering from the Korea Advanced Institute of Science and Technology, Daejeon, South Korea, in 1998 and 2002, respectively. He was a Visiting Scientist at the National Institute of Standards and Technology (NIST), Boulder, CO, USA, in 2010. From 2002 to 2005, he was a Senior Research Engineer at the Devices and Materials Laboratory, LG Electronics Institute of Technology, Seoul, South Korea. He has been with the Korea Research Institute of Standards and Science, Daejeon, since 2005, where he is currently the Head of Electromagnetic Wave Metrology Group and a Principal Research Scientist. Since 2013, he has been a Professor with the Science of Measurement Department, University of Science and Technology, Daejeon. His current research interests include electromagnetic power, impedance, and antenna measurement. He is a Life Member of the Korea Institute of Electromagnetic Engineering and Science (KIEES) and a member of IEICE.